Nanoscale Flow Choking at the Zero Slip Length: Universal Benchmark Data for In Silico Experiments

V R Sanal Kumar (vr_sanalkumar@yahoo.co.in)
Indian Space Research Organisation https://orcid.org/0000-0002-5643-7223

Vigneshwaran Sankar
Indian Institute of Science

Nichith Chandrasekaran
Indian Institute of Science Bangalore

Sulthan Ariff Rahman Mohamed Rafic
Kumaraguru College of Technology

Ajith Sukumaran
Kumaraguru College of Technology

Bharath R.S.
Indian Institute of Science Bangalore

Charlie Oommen
Indian Institute of Science Bangalore

Pradeep Kumar Radhakrishnan
GITAM University

Shiv Kumar Choudhary
All India Institute of Medical Sciences

Article

Keywords: Sanal flow choking, DDT, Nanoscale system, Zero slip length, No slip boundary condition, diabatic nanoscale flows, boundary layer blockage

Posted Date: November 11th, 2020

DOI: https://doi.org/10.21203/rs.3.rs-94923/v1

Nanoscale Flow Choking at the Zero Slip Length: Universal Benchmark Data for *In Silico* Experiments

An Exact Prediction of the 3D Blockage Factor in Nanoscale Systems

V.R.Sanal Kumar,[1-3,*] Vigneshwaran Sankar,[2,3] Nichith Chandrasekaran,[2,3] Sulthan Ariff Rahman Mohamed Rafic,[3] Ajith Sukumaran,[3] R.S.Bharath,[2] Charlie Oommen,[2] Pradeep Kumar Radhakrishnan,[4] Shiv Kumar Choudhary[5]

[1]*Indian Space Research Organisation, VSSC, Trivandrum 695 022, Kerala, India*
[2]*Indian Institute of Science, Bangalore, Karnataka, 560012, India*
[3]*Kumaraguru College of Technology, Coimbatore – 641 049, Tamil Nadu, India*
[4]*GITAM University, Visakhapatnam– 530045, Andhra Pradesh, India*
[5]*All India Institute of Medical Sciences, New Delhi – 110608, India*

[*]***Corresponding Author:*** Email: vr_sanalkumar@yahoo.co.in, Phone: +91-8754200501

The *Sanal flow choking* (PMCID: PMC7267099) and the *streamtube* flow choking are new theoretical concepts applicable to both the continuum and non-continuum fluid flows. Once the streamlines compacted, the considerable pressure difference attains within the streamtube and the flow within the streamtube gets accelerated to the constricted section for satisfying the continuity condition set up the conservation law of nature, which leads to the *Sanal flow choking* and supersonic flow development at a critical-total-to-static pressure ratio (CPR) due to the convergent-divergent (CD) shape of the streamtube. As the pressure of the *nanofluid*/non-continuum-flows rises, *average-mean-free-path* diminishes and thus, the *Knudsen number* lowers heading to a zero-slip wall-boundary condition with compressible viscous (CV) flow regime. *Sanal flow choking* is a CV flow phenomenon creating a physical situation of the *sonic-fluid-throat* in a duct at a CPR. Herein, we presented a closed-form-analytical-

model, which is capable to predict exactly the three-dimensional boundary-layer-displacement-thickness of *nanoscale* diabatic fluid flow (*flow involves transfer of heat*) systems at the zero-slip-length. The innovation of *Sanal flow choking* model is established herein through the entropy relation, as it satisfies all the conservation laws of nature. The exact value of the 3D boundary-layer-displacement-thickness in the *sonic-fluid-throat* region presented herein for each gas is a universal benchmark data for performing high-fidelity *in vitro* and *in silico* experiments for the lucrative design optimization of *nanoscale* systems. The physical insight of the *Sanal flow choking* and *streamtube* flow choking presented in this letter sheds light on finding solutions for numerous unresolved scientific problems.

Key words: Sanal flow choking, DDT, Nanoscale system, Zero slip length, No slip boundary condition, diabatic nanoscale flows, boundary layer blockage.

The theoretical finding of the *Sanal-flow-choking* [1,2] is a methodological advancement in the modeling of the continuum and non-continuum real-world composite fluid flows at the creeping-inflow (low subsonic flow) conditions. The closed-form analytical model conceiving all the conservation laws of nature at the *Sanal flow choking* condition for *diabatic* flow is certainly the unique scientific language of the Universe, which we are presenting herein for solving various unresolved problems carried forward over the centuries. Cognizing physics of multi-phase and multi-species fluid flows and controlling the composite flow at the *nanoscale* is vital for inventing, manufacturing, and lucrative performance improvements of nano-electro-mechanical systems (NEMS) for high precision applications[3-10]. The design of such systems are currently a subject of great interest in aerospace industries. This is particularly true for the design optimization of certain aerospace systems in the international space station (ISS) and nanoscale

thrusters[11] operating at both gravity and microgravity environments where the flow field exhibit both the continuum and non-continuum fluid properties. In such physical situations multiscale and hybrid modeling approaches are encouraged[12]. Although the mathematical modeling and high-fidelity *in silico* simulation of physics of non-continuum/*nanofluid* flow is progressed substantially over the last few decades there are numerous unanswered research questions in *real-world fluid flows*[1-10] for a plausible judgment on the space systems design. One such problem of paramount interest is for performing *in silico* and *in vitro* experiments for the design optimization of aerospace propulsion devices. Therefore, it is inevitable for capturing flow physics of high-pressure composite creeping fluid flow passing through a convergent-divergent (CD) duct, facilitated with a *nanoscale* throat with *microscale* length (see Fig.1(a)), featuring both continuum and the non-continuum fluid flow properties.

Nanofluid flow is a blend of *nano-sized particles* in a traditional operating fluid[12], which obeys all the conservation laws of nature. The occurrence of slip in gas flows, due to the local thermodynamic non-equilibrium, was originally reported by Maxwell[14,15] and its scale varies on the extent of rarefaction of the gas. It describes in terms of the *Knudsen number* (*Kn*), which gives an explicit clue on the type of flow, viz., continuum or non-continuum. Note that numerous modeling efforts have been reported in the open literature for *nanoscale* flow simulation without authentic code verification using any benchmark data and/or any closed-form analytical solution[16-35]. The fact is that generating benchmark data from the *nanoscale* system is a challenging task or quite impractical using a conventional *in vitro* methods and it is anticipated that the classical assumptions on the hydrodynamic model will ride into hitches as the composite flow system reaches nanometer (nm) size.[19] Obviously the brilliant conclusions drawn using sophisticated models, by various investigators across the globe, viz., direct simulation Monte

Carlo (DSMC), molecular dynamics (MD), Burnett equation and the hydrodynamic models, will not be endorsed by the high precision industries for the highly expensive *nanoscale* systems designs for practical applications without providing an exact solution for the data verification. Cooper et al.[19] reported that *in vitro* data well matched with the predicted results using the

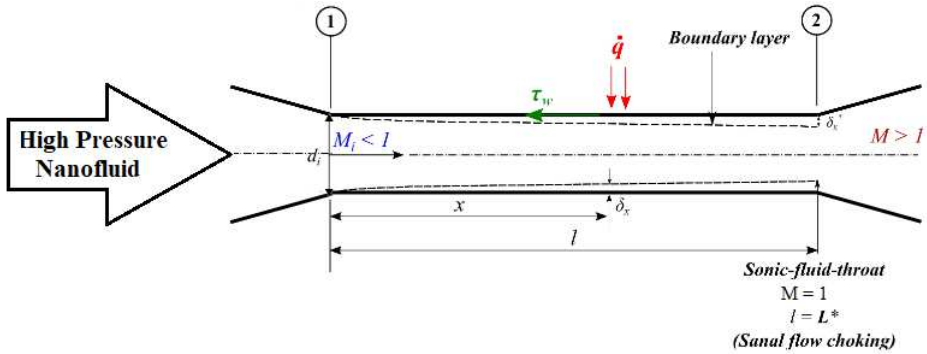

Fig. 1(a) Demonstrating the *Sanal flow* choking condition in an idealized physical model of an internal *nanoscale fluid* flow system.

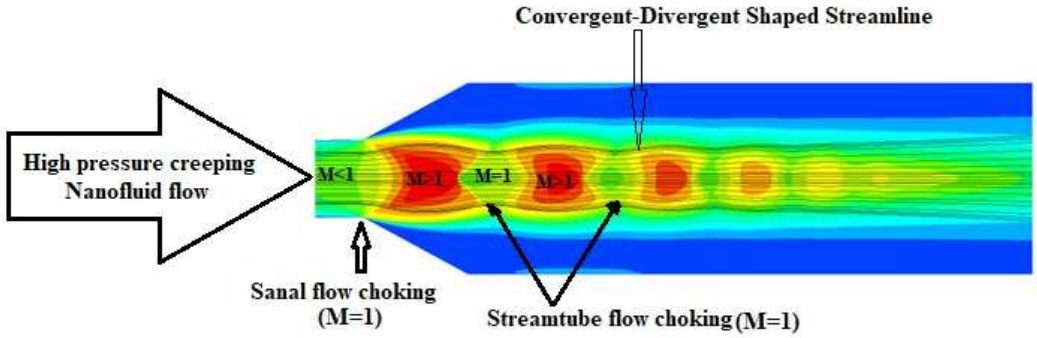

Fig. 1(b) Demonstrating the *Sanal flow* choking and streamtube flow choking condition in an idealized physical model of an internal *nanoscale fluid* flow system.

hydrodynamic Navier Stokes method with the first-order slip condition for the range of average pore diameters from 169-220 nm. Singh and Myong[36] reported that neither continuum models nor free-molecular models could be invoked for fluid flow cases when the *Knudsen number* falls in the intermediate range between the continuum ($Kn \leq 0.01$) and free-molecular flow regimes ($Kn \geq 10$). When the *Knudsen number* becomes large ($Kn > 0.01$), the conventional assumptions of no-slip boundary condition, thermodynamic equilibrium, and linear stress-strain relationship

fail. Admittedly, when the pressure of the *nanofluid* rises, the *average-mean-free-path* diminishes and thus, the *Knudsen number* lowers heading to a zero-slip wall-boundary condition with compressible viscous (CV) flow regime creating *streamline* pattern in the *nanoscale* fluid flow system. Therefore, the *Sanal flow choking* and supersonic flow development leading to shock-wave generation due to the *fluid-throat* effect at the zero-slip-length is a valid physical situation in continuum and non-continuum flows where CD shaped nanoscale *streamtubes* persists (see Fig.1(b)). Herein, we provide a proof of the concept of *fluid-throat* persuaded flow choking in the nanoscale *diabatic fluid flow* system. For establishing this concept authoritatively, we are presenting an infallible closed-form analytical model for predicting the three-dimensional (3D) boundary layer displacement thickness (defined herein as 3D blockage factor) at the *sonic-fluid-throat* location where the slip length is zero, which will be a useful tool for the *in vitro* and *in silico* experiments in both the continuum and non-continuum flows with due consideration of heat transfer effects (real-world fluid flow effect).

D.M.Holland et al.[37] reported that an *in silico* model enhanced with molecular-level information could accurately predict unsteady *nanoscale* flows in non-trivial geometries. Authors presented that slip at the nanoscale fluid flow system could make a noteworthy effect on the optimum channel dimensions; and formulated an analytical equation which corrects the well-known Murray's Law.[38] It was reported that for a given cavitation resistance throughout the xylem network, Murray's law should apply, which predicts the optimal taper of viscoelastic vessels.[38-41] While searching for singularities in the Navier–Stokes equations Terence Tao[42] reported that the partial differential equations that describe nonlinear effects of several cases are inadequately realized. Moseler and Landman[43] used molecular dynamics (MD) simulations of nanoscale jets to encounter a rupture profile not illustrated by macroscopic theory. Of late

(2020), Chengxi Zhao[44] reported that the soundness of the traditional theories at the microscale and nanoscale has been taken into question. Authors reported that the thermal fluctuations are spontaneously occurring within molecular dynamics (MD) simulations. D.M.Holland et al.[37] further reported that the time dependent mass flow rate predicted using their enhanced computational fluid dynamics (CFD) simulation matches well with full molecular dynamics (MD) simulation and highlighted that the traditional CFD results of such cases are incompetent. It leads to say that in real world scientific experiments of complex nano-microscale systems the robustness of *in silico* model needs to be tested to featuring the actual fluid characteristics in a non-trivial geometry at the *nanoscale*. Singh and Myong [36] reported that for improved modeling efforts, the joint effect of material properties, the scale and shape of the flowing medium on fluid flow must be taken into account, which is lacking now and we are addressing it through the closed-form analytical models.

It is an admitted fact that all the fluids in nature are compressible because the specific heat at the constant-pressure (C_p) is always higher, ranging from a zero-plus (0+) value, than the specific heat at the constant-volume (C_v) of all real-world fluids.[1] The traditional assumption of taking water as an incompressible fluid[10-27] is patently not true as its specific volume (or density) does change with temperature and/or pressure.[1]

The exact prediction of the 3D blockage factor throughout the flow field is a meaningful objective of any fluid flow system design from *yocto* to *yotta* scale and beyond, which is still an unresolved problem. Of late V.R.S.Kumar et al.[1,2] exactly predicted the 3D blockage factor in the *sonic-fluid-throat* region at the Sanal flow choking condition. The real scientific fact is that the *Sanal flow choking* is a *compressible* fluid flow effect, which occurs in any duct with uniform port geometry, due to the boundary layer blockage induced internal flow choking at a critical-

total-to-static pressure ratio (CPR), as the boundary layer blockage factor will never be zero in any real-world flows.[45] The critical TSPR for flow choking of composite fluids would vary based on the lowest heat capacity ratio (HCR) of the evolved species at the constriction region (*fluid-throat*) of the *streamtube* (see Fig.1(b)). Note that the molecular dynamics condition in the composite fluid flow system could alter the streamline-pattern at different time and location. Therefore, pinpointing the exact location of *streamtube* flow choking is a challenging *in vitro* and *in silico* topic of great interest to the nano-microscale system designers.

RESULTS AND DISCUSSION

Herein, we presented an exact solution of the 3D blockage factor with molecular precision at the condition prescribed by the *Sanal-flow-choking* for diabatic fluid flows, which is an authorized benchmark data for the verification of the results generated from *in vitro* and *in silico* experiments of real-world nanoscale fluid flow problems. The innovation of the *Sanal-flow-choking* model is established herein through the entropy relation, as it satisfies all the conservation laws of nature. The beauty and novelty of the closed-form analytical model presented herein stem from the veracity that at the *Sanal flow choking* condition for *diabatic nanoflows*, all conservation laws of nature are satisfied in the unique *sonic-fluid-throat* location. In this letter analytical models are presented for establishing the causes and effects of the *Sanal flow choking* in an internal nanoscale fluid flow system with sudden expansion or divergent region. This was an unresolved world-wide scientific problem for more than a century.

Note that in general any fluid flow system from *yocto* to *yotta* scale and beyond with sudden expansion or divergent region (see Fig.1(a-b)) could create the physical situation of the *Sanal flow choking* at a CPR, which is regulated by HCR (γ) as dictated by Eq.1. The 3D non-dimensional blockage factor (3DNBF) in an internal flow system with the cylindrical upstream-

duct is derived from the compressible fluid flow theory[2, 46] and presented herein as Eq.2(a-b) for *diabatic* nanoscale flow systems with a desirable inflow condition (see Eq.3). At the *Sanal flow choking* condition, the 3D blockage factor (3DBF) at the *sonic-fluid-throat* ($M_{axial} = 1$) is derived and presented herein as Eq.2(b), which is the highest blockage factor in the internal-multispecies-choked-*nanoscale* fluid flow system.

$$CPR = \left(\frac{(HCR)_{\substack{evolved\ gases \\ with\ the\ lowest\ HCR}} + 1}{2} \right)^{(HCR)_{lowest} / (HCR)_{lowest} - 1} \tag{1}$$

$$3DNBF\Big|_{\substack{@\,the\,upstream\ port \\ of\ the\ nanoscale\,system}} = \frac{2\delta_x}{d_{inlet}} = 1 - \left[\frac{M_{\mathbf{inflow}}}{M_{axial}} \right]^{1/2} \left[\frac{1 + \frac{\gamma - 1}{2} M_{axial}^2}{1 + \frac{\gamma - 1}{2} M_{\mathbf{inflow}}^2} \right]^{\frac{\gamma + 1}{4(\gamma - 1)}} \tag{2a}$$

$$3DBF\Big|_{@\,sonic-fluid-throat} = \left[1 - M_{\mathbf{inflow}}{}^{1/2} \left[\frac{2}{\gamma_{highest} + 1} \left(1 + \frac{\gamma_{highest} - 1}{2} M_{\mathbf{inflow}}^2 \right) \right]^{\frac{\gamma_{highest} + 1}{4(1 - \gamma_{highest})}} \right] d_{inlet\ port} \tag{2b}$$

$$\frac{1 + \gamma_{lowest}}{1 + \gamma_{lowest} M_{inflow}^2} = \left(\frac{\gamma_{lowest} + 1}{2} \right)^{\frac{\gamma_{lowest}}{\gamma_{lowest} - 1}} \tag{3}$$

It is pertinent to highlight here that the model set for *Sanal flow choking* for real-world fluid flows, the inflow Mach number (M_i) must be selected based on the *thermal choking* (*Rayleigh flow* effect) condition as dictated by Eq.3. Note that the chances of *Sanal flow choking* increases when

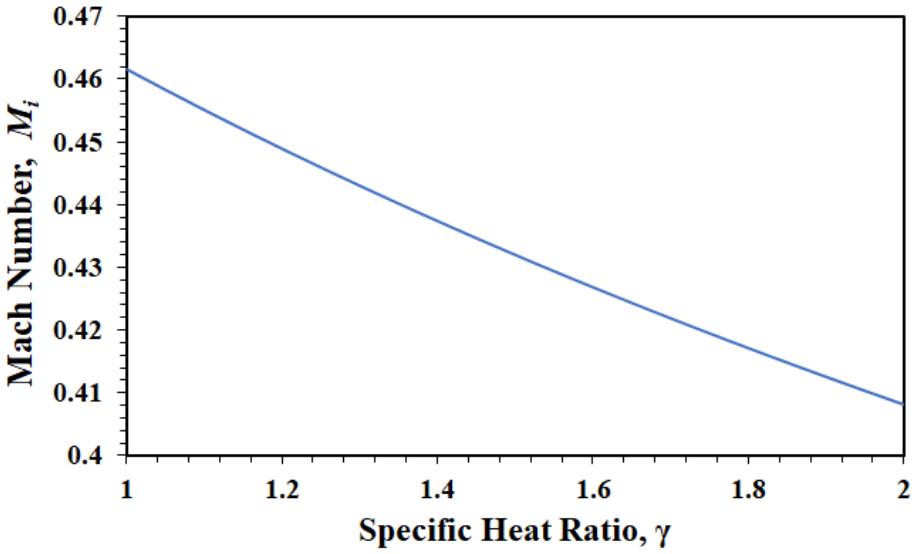

Fig. 2(a) Inlet Mach number prediction of different gases with different HCR (γ) for achieving *Sanal flow choking* condition for *diabatic nanoflows*.

the HCR of gases decreases due to the decreases in CPR of the nanoscale flow system as dictated by Eq.1. The solution curve of Eq.3 is presented as Fig.2(a). While performing the *in silico* model verification and calibration, the *average friction coefficient* must be chosen in accordance with the *Fanno flow choking* condition.[2,46] Admittedly, at the *sonic-fluid-throat* of the *nanoscale* fluid flow system (see Fig.1(a-b)), the *thermal choking* and the wall-friction induced flow choking converges and satisfy all the conservation laws of nature.

In the *in silico* study the *average friction coefficient* ($\bar{f}$) may be estimated from Eq.4 based on the lowest HCR (γ_{lowest}) of the evolving gases for satisfying the condition set for the *Sanal flow choking* for real-world multiphase, multi-species *nanoscale fluid*-flow systems.

$$\bar{f} = \frac{d_i}{4L^*}\left[\frac{1-M_i^2}{\gamma_{lowest}M_i^2}+\frac{\gamma_{lowest}+1}{2\gamma_{lowest}}\ln\left[\frac{(\gamma_{lowest}+1)M_i^2}{2+(\gamma_{lowest}-1)M_i^2}\right]\right] \quad (4)$$

where $\bar{f}$ is an average friction coefficient[46] termed as (see Eq.4(a)),

$$\bar{f} = \frac{1}{L^*}\int_0^{L^*} f\, dx \qquad (4a)$$

The solution curve of Eq.4 is given in Fig.2(b) in the semi-log plot.

Note that the dominant species with the lowest HCR predisposes for an early *Sanal flow choking* at the sudden expansion or transition region of any internal flow system (see Fig.1(a-b)). Note that Eqs. 1-5 are useful mathematical models for the high-performance aerospace chemical systems architects for predicting the limiting condition of *deflagration to detonation transition* (DDT) in nanoscale thrusters with confidence. Further discussion pertaining to the nanoscale chemical system design is beyond the scope of this letter. This letter is set for predicting the benchmark data at the *Sanal flow choking* condition for *in vitro* and *in silico* experiments in *nanoscale* fluid flow systems for various applications.

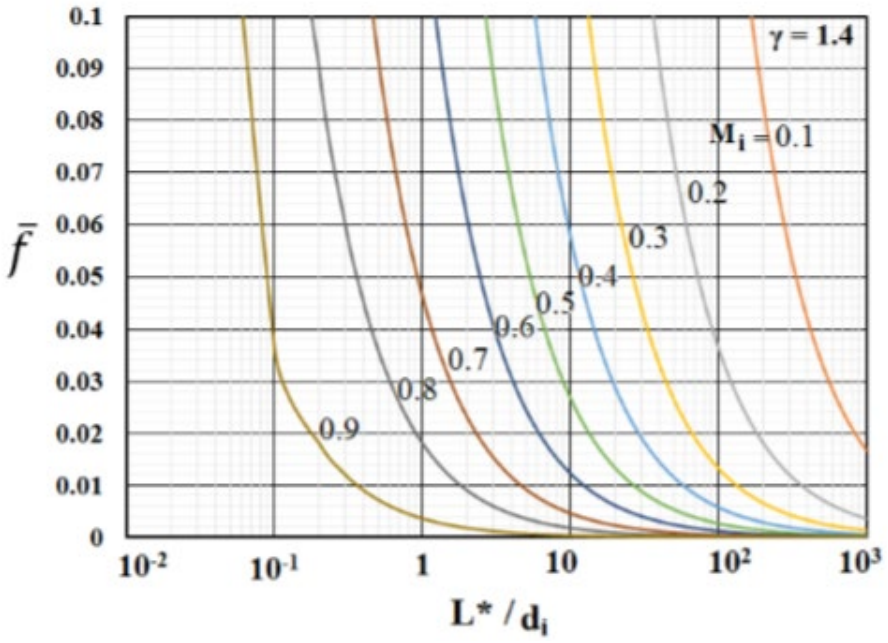

Fig. 2(b) Analytical prediction of the *average friction coefficient* at the *Sanal flow choking* condition of different nanotubes at different inlet conditions.

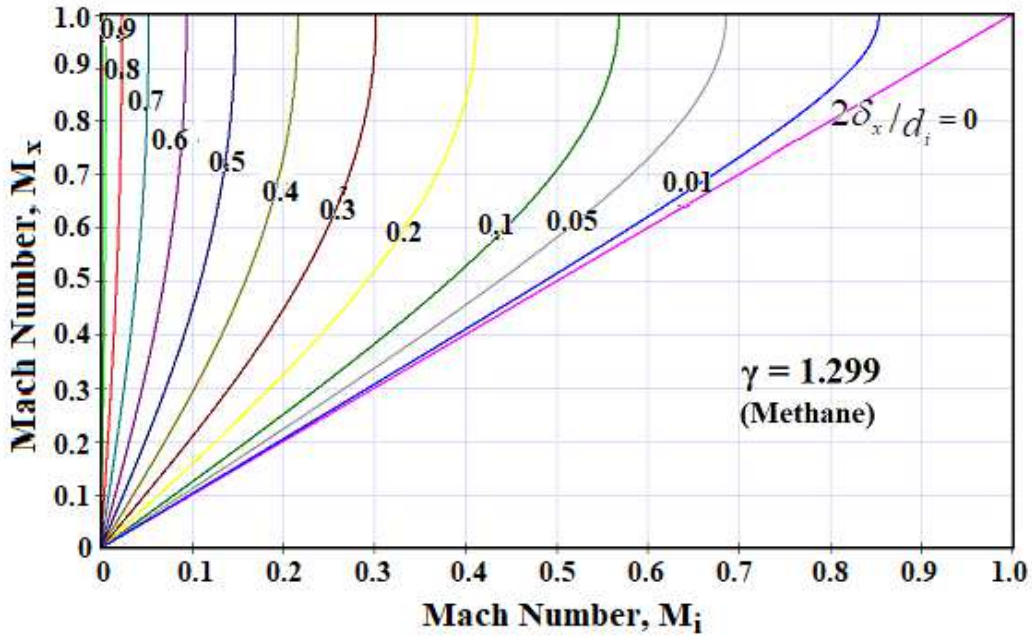

Fig. 2(c) The solution curve of Eq.2(a) showing the 3D blockage factor with *Methane* as the working fluid.

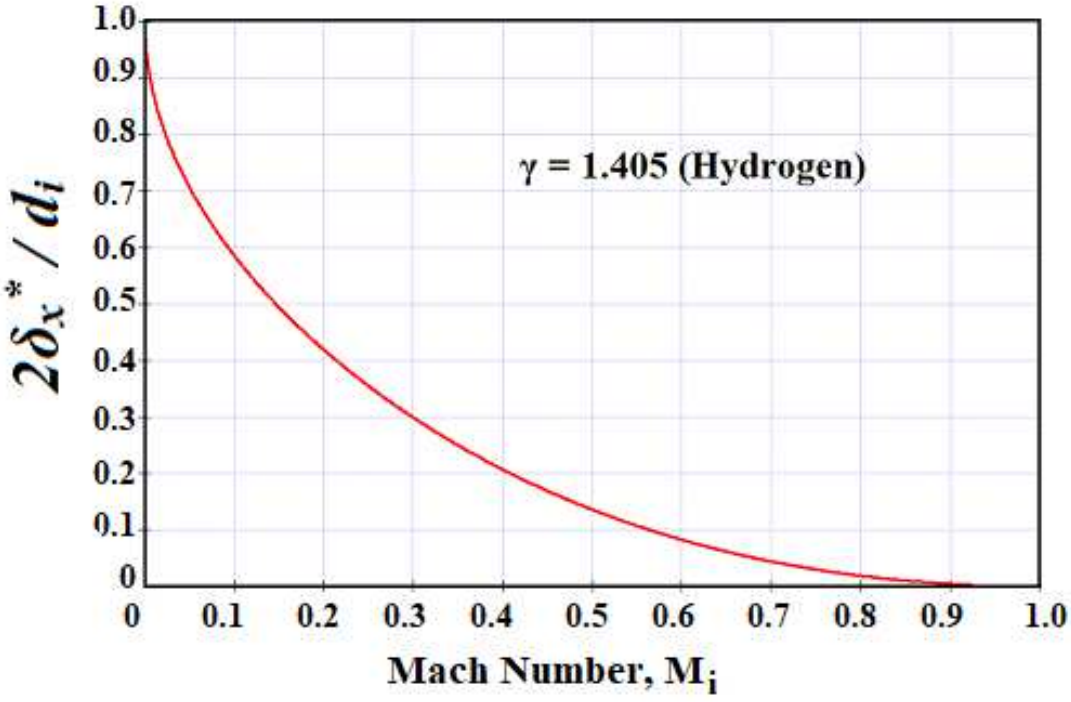

Fig. 2(d) The solution curve of Eq.2(b) showing the 3D blockage factor at the *sonic-fluid-throat* of a *nanofluid* flow system with hydrogen as the working fluid.

Vigneshwaran's Table (Table-1) gives the exact values of 3DNBF at the *Sanal flow choking* condition of seven different working gases and the corresponding CPR and inlet Mach number. The CPR value is an indication of the lower critical detonation index (LCDI) of the internal flow systems having accumulated with such types of gases. The 3DNBF is a very useful benchmark data for nanoscale *in vitro* experiments and *in silico* model verification, validation and calibration with credibility, which was an unresolved problem over centuries. The corresponding non-dimensional blockage factor for two-dimensional[2] case is also given in Table-I for comparison at the *Sanal flow choking* condition for real-world flows. The solution curve of Eq.2(a) for Methane gas is given in Fig.2(c) and the solution curve of Eq.2(b) for Hydrogen gas is depicted in Fig.2(d).

It is important to note that, at the *sonic-fluid-throat* of any wall-bounded real-world flows, all the three flow choking conditions, viz., *Sanal flow choking*[1,2]*, Rayleigh flow choking*[46] and *Fanno flow choking* [45] converges due to the prudent boundary conditions set herein for generating *benchmark data*. It is pertinent to note that the magnitude of the *entropy* of these three flow choking models are different at the sonic condition. The entropy relationship developed for the *Sanal flow model* altogether conceived the *Rayleigh flow* model and *Fanno flow* model effects and presented herein as Eq.6.

$$\left(\frac{s_2 - s_1}{C_p}\right)_{Sanal\ Flow} = \ln\left[\left(\frac{M_2}{M_1}\right)^{3\gamma_{lowest}-1/\gamma_{lowest}}\left(\frac{1+\gamma_{lowest}M_1^2}{1+\gamma_{lowest}M_2^2}\right)^{\gamma_{lowest}+1/\gamma_{lowest}}\left(\frac{1+\frac{\gamma_{lowest}-1}{2}M_1^2}{1+\frac{\gamma_{lowest}-1}{2}M_2^2}\right)^{\gamma_{loest}+1/2\gamma_{lowest}}\right] \quad (6)$$

The analytical solution of the Entropy-Mach relationship (see Eq.6) for the *Sanal flow choking* model for the *nanoscale fluid* flow system is compared with the *Fanno* flow and *Rayleigh* flow models and presented in Fig.2(e) with air as the operating fluid. It is apparent from

Fig.2(f) that the change in entropy is obtained as zero at $M_1 = M_2 = 1$, which is validating the capability of the model for meeting the *Sanal flow choking* condition for the *nanoscale fluid* flow systems for benchmarking the data reported in Table-1. It could be taken as the authenticated data for elucidating high fidelity wall-bounded nanoscale fluid flow problems in various industrial applications. Attaining the *Sanal flow choking* effect in *diabatic nanoscale* fluid flow systems, the inlet Mach number needs to be estimated using Eq.3 related to the HCR (γ) of the operating fluid (see Table-1 & Fig.2(a)). The LCDI presented in Table-1 is a powerful indicator of knowing the *detonation* index of nanoscale chemical energy systems with sudden expansion or divergent port for prohibiting the catastrophic failures due to the *Sanal flow choking* and/or *streamtube flow choking (see Fig.1(b))*.

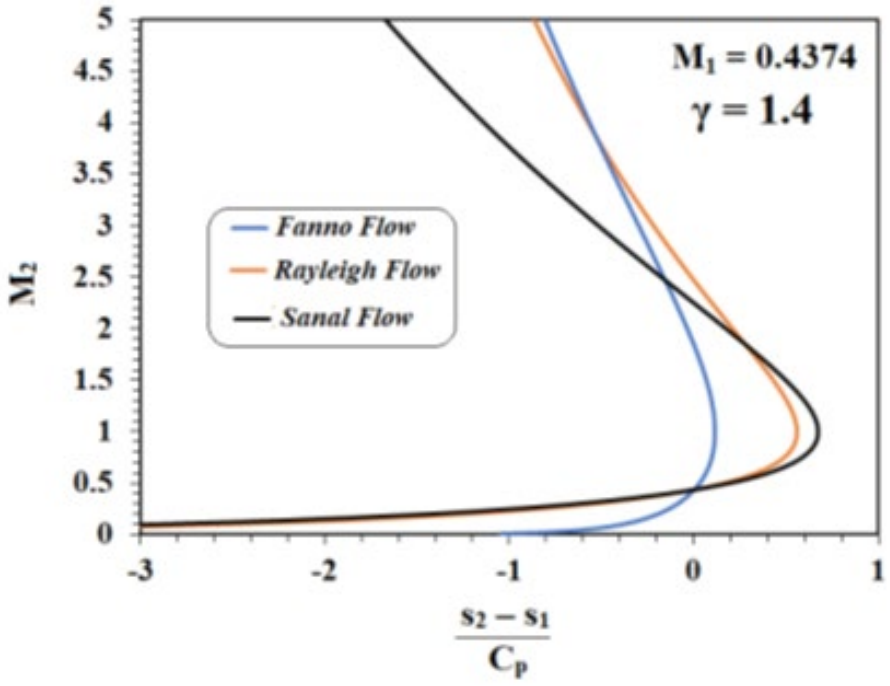

Fig. 2(e) Mach Number-Entropy chart of *Fanno, Rayleigh* and *Sanal* flow models at the choked flow condition.

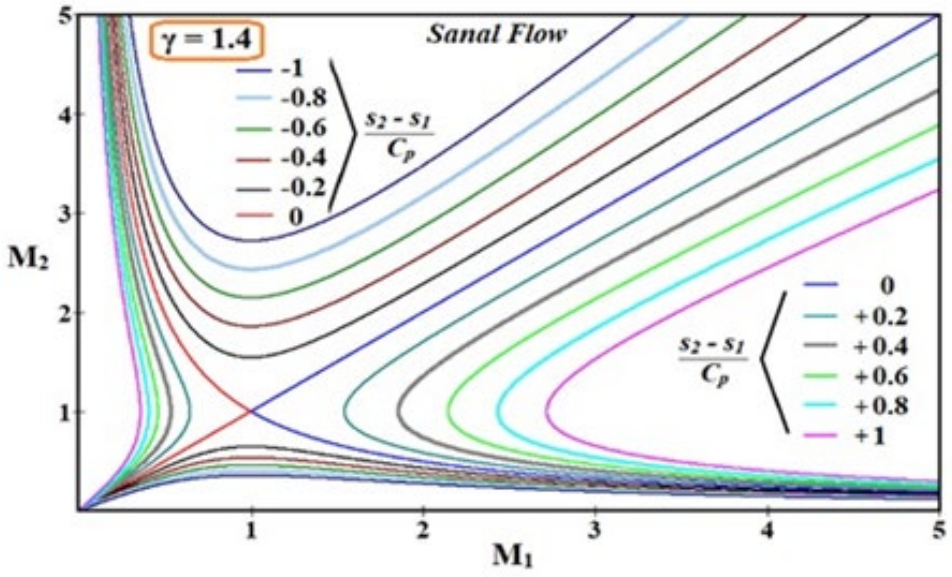

Fig. 2(f). The demonstration of the *Sanal flow choking* in *diabatic nanofluid* flows. (Solution curves of Eq. 6).

It is pertinent to state that, as seen in Table-1, the three-dimensional blockage factor is always lower than the two-dimensional blockage factor of any wall-bounded *nanoscale fluid* flow system at the *Sanal flow choking* condition. Note that *nanoscale fluid* flow system must always maintain the flow *Mach number* less than one as dictated by Eq.7 and Eqs.7(a-c) for negating the undesirable *Sanal flow choking* and *streamtube flow choking* causing shock wave generation and pressure-overshoot. Eqs.7(a-c) are different forms of Eq.7, which are useful for deciding the *thermophysical* properties of *nanomaterials* and the corresponding base fluid for various nanoscale system developments and its applications.

$$M_{nanofluid} < 1 \qquad (7)$$

$$\frac{\text{Fluid flow rate}}{\text{Vessel cross sectional area}} \sqrt{\frac{(\text{Prandtl Number})\,(\text{Thermal Conductivity})}{(\text{HCR})\,(\text{Density})(C_p)\,(\text{Dynamic Viscosity})\,(\text{Static Pressure})}} < 1 \qquad (7a)$$

$$\frac{\textbf{Nanofluid flow rate}}{\textbf{Vessel cross sectional area}}\sqrt{\left(\frac{\mathrm{Pr}}{\mathrm{Nu}}\right)_{nanofluid}\frac{\left(h_x\right)_{nanofluid}\;\;x_{BL\,length}}{\gamma_{nanofluid}\,\rho_{nanofluid}\left(C_p\right)_{nanofluid}\mu_{nanofluid}\,P_{static}}}\;<\;1 \qquad (7b)$$

$$\frac{Re_{nanofluid}\,\nu_{nanofluid}}{d_H}\left[\frac{\rho_{nanofluid}}{\gamma_{nanofluid}\left(P_{static}\right)_{nanofluid}}\right]^{1/2}<\;1 \qquad (7c)$$

The self-explanatory equations (see Eq.7(a-c)), derived from the compressible flow theory, are highlighting herein for demonstrating the various influencing parameters and the conflicting requirements to prohibit the *Sanal flow choking* in the *nanoscale fluid* flow system. Eq.7(a) reveals that a disproportionate increase of the *thermal conductivity* of *nanofluid* increases the risk of *Sanal flow choking* leading to supersonic flow development followed by shock wave and pressure-overshoot in the nanoscale flow systems with sudden expansion or divergent region (see Fig.1(a-b)). Therefore, the condition set by Eq.7(a) must be satisfied while addition *nanomaterials* in the base fluid for reducing the risk of catastrophic failure of *nanoscale propulsion* systems. Furthermore, here we show through Eq.7(b) that while decreasing the whole-viscosity of the composite flow for prohibiting the Sanal flow choking, the *Reynolds number (Re)* increases and the laminar flow could be disrupted and becomes turbulent causing an early *Sanal flow choking* in the creeping inflow condition. Therefore, *in vitro* parametric studies of aerospace propulsion systems in ISS must be carried out with caution because relatively high and low fluid viscosity are risk factors for the *Sanal flow choking*. The coupled influence of various parameters of nanoscale fluid flow systems leading to the *Sanal flow choking* condition are, flow rate, Prandtl number (*Pr*), Nusselt number (*Nu*), Reynold number (*Re*), thermal conductivity, heat capacity ratio $\left(\gamma_{nanofluid}\right)$, density $\left(\rho_{nanofluid}\right)$, dynamic viscosity $\left(\mu_{nanofluid}\right)$,

kinematic viscosity $\left(\nu_{nanofluid}\right)$, static pressure ($P_{static}$), specific heat at constant pressure $\left(C_P\right)_{nanofluid}$, hydraulic diameter of the duct (d_H), convective heat transfer coefficient $\left(h_x\right)_{nanofluid}$, and the characteristic length in the direction of growth of the boundary layer $\left(x_{BL\,length}\right)$. Please note that the coupled influence of the above-listed parameters will be controlled by a unique property of the *nanofluid*, which is stated herein with brevity as the heat capacity ratio (HCR) of *nanofluid* as dictated by Eq.1. This is a remarkable finding for the nanoscale systems development.

Viscosity variations are depending on the shear rate or shear rate history of the fluid, which could vary due to the variations in the *thermophysical* properties of *nanomaterials* and local *effects* too. The boundary-layer-blockage factors presented in Table-1 (the solution of Eq.2(b)) and the average friction coefficient given in Table-II (the solution of Eq.4) for different gases are the authenticated benchmark data generated from the closed-form analytical models for conducting *in silico* experiments after due verification, validation and calibration of the corresponding *in silico* models with *nanomolecular* precision with credibility. The benchmark data at the *Sanal flow choking* condition for *diabatic* flows for both *base fluid* and *nanofluid* presented in Table-1 and Table-2 are useful to the nanoscale system designers for enormous interdisciplinary bids.

Several *in vitro* and *in silico* experiments were reported by other investigators for examining the heat transfer performance of different *nanofluids* with different *thermophysical* properties through the traditional verification, validation and calibration of *in silico* models. Although the published *in silico* results are interesting, the accuracy of the data generated through *in silico* modeling efforts, typically do for the physical and chemical industry problem solutions, are not sufficient to authorize *nanoscale* systems design for manned space missions or *in vitro* studies in ISS. The fact is that those *in silico* models were not used any reliable benchmark data or any

exact solution obtained from the closed-form analytical models, which we could resolve herein. Certainly, a well-calibrated fluid-structural, multi-phase, and the multi-species *in silico* model at the condition prescribed by the closed-form analytical model, presented herein for the *Sanal flow choking* for *diabatic nanofluid*, could generate a reliable database for examining the effectiveness of dispersing *nanometer-sized* materials in the base fluids for a credible decision making on the desirable characteristics of *nanofluids* for various nanotechnology applications. It is important to note that while adding *nanometer-sized materials* to the base fluid the HCR of the *nanofluid* should not decrease. Note that a decrease in HCR leads to an early *Sanal flow choking* leading to shock wave generation and pressure-overshoot in the nanoscale system owing to the fact that the value of CPR will decrease while decreasing the HCR.

In light of the above observations the risk and benefits of *nanofluids* can be examined for various industrial applications through multiphase, multispecies *in silico* experiments by performing reliable parametric analytical studies by varying size, shape, volume and mass concentration, and thermophysical properties of *nanomaterials* in any base fluid. It is appropriate to mention here that the *Sanal flow choking* is an undesirable phenomenon in any *internal flow system* as it generates shock waves and inherent pressure-overshoot, which could alter the thermoviscoelastic properties of the vessel wall. The consequence of the *Sanal flow choking* is more severe if the duct geometry is having sudden expansion, the divergent/bifurcation region, expansion values or CD nozzle passage effect. In such duct flows the creeping flow gets accelerated to supersonic flow, at a CPR for flow choking, for meeting the conservation laws of nature.[1,2] It has been well proven over the years that, in accordance with the law of nature, any minor disturbance to the supersonic flow leads to the shock-wave generation in the downstream region of the duct leading to the causation of pressure-overshoot in the downstream region

inviting *memory effects* on the viscoelastic walls of the duct. This is a grey area, which needs to be examined in detail through fluid-structural interactive multiphase, multispecies *in silico* models, which is beyond the scope of this letter.

CONCLUSIONS

The Sanal flow choking model presented herein is useful for *in vitro* and *in silico* experiments of all real world fluid flow problems (continuum / non-continuum). Although the interdisciplinary science of nanotechnology has been advanced significantly over the last few *decades* there were no closed-form analytical models to predict the 3D blockage factor of *diabatic nanoscale fluid flow system*. The *Sanal flow choking* for the diabatic condition presented herein is valid for all the real-world fluid flow problems for designing various *nanoscale fluid* flow systems and sub systems due to the fact that the model is untied from empiricism and any types of errors of discretization. Using Eq.1 and Eq.2 the chemical propulsion system designers could easily predict the likelihoods of *detonation* with the given inlet flow Mach number and the lowest value of the HCR of the leading gas coming from the upstream port of the chemical system.[47] In a nutshell, the best choice of increasing the solid fuel loading in the nanoscale thruster design without inviting any undesirable *detonation* and catastrophic failures, is to increase the HCR of the working fluid. Further discussion on the nanoscale propulsion system design is beyond the scope of this letter.

We have established herein that, due to the evolving boundary layer and the corresponding area blockage in the upstream port of any internal *nanofluid* flow system with sudden expansion or divergent region, the creeping *diabatic nanoflow* ($M_i << 1$) originated from the upstream port of the system could accelerate to the supersonic flow leading to an undesirable phenomenon of

pressure-overshoot due to shock wave generation as a result of the *Sanal flow choking.* Through the proposed mathematical methodology, we could disprove the general belief of the impossibilities of internal flow choking in such real-world *nanoscale fluid* flow systems at the creeping inflow conditions. There was a general belief in the scientific community over the centuries that the subsonic/creeping flow would not be augmented up to supersonic flow without shipping through a geometric throat, which we have disproved herein through the closed-form analytical model. Note that if the total-to-static pressure ratio at the *fluid-throat* is lower than the LCDI the *detonation* would not occur even if the blockage factor is relatively high in nanoscale chemical propulsion systems. The physical insight of the *Sanal flow choking* and *streamtube* flow choking presented in this letter sheds light on finding solutions for numerous unresolved scientific problems carried forward over the centuries in physical, chemical and mechanobiological sciences.

METHODS

Closed-form analytical methodology <https://doi.org/10.1063/1.5020333>.

Acknowledgment

Science and Engineering Research Board of the Department of Science and Technology, the *Government of India* for providing grant (File No. ITS/2018/002316).

References

1. V.R.Sanal Kumar, Vigneshwaran Sankar, Nichith Chandrasekaran, Ajith Sukumaran, Sulthan Ariff Rahman Mohamed Rafic, Roshan Vignesh Baskaran, R.S.Bharath, Charlie Oommen, Pradeep Kumar Radhakrishnan, Shiv Kumar Choudhary, "Sanal Flow Choking: A Paradigm Shift in Computational Fluid Dynamics Code Verification and Diagnosing Detonation and Hemorrhage in Real-World Fluid-Flow Systems," Global Challeges, A Wiley Publication, May 2020, https://doi.org/10.1002/gch2.202000012, https://pubmed.ncbi.nlm.nih.gov/32837737/
2. V.R. SanalKumar et al., "A closed-form analytical model for predicting 3D boundary layer displacement thickness for the validation of viscous flow solvers," *AIP Advances,* **8**, 025315 (2018), pp.1-22, ; doi: 10.1063/1.5020333; https://doi.org/10.1063/1.5020333.
3. Whitby, M., Quirke, N. Fluid flow in carbon nanotubes and nanopipes. *Nature Nanotech* **2,** 87–94 (2007). https://doi.org/10.1038/nnano.2006.175
4. The risks of nanomaterial risk assessment. *Nature Nanotech.* **15,** 163 (2020). https://doi.org/10.1038/s41565-020-0658-9
5. Matsumoto, Y., Nichols, J. W., Toh, K., Nomoto, T., Cabral, H., Miura, Y., Kataoka, K. (2016). *Vascular bursts enhance permeability of tumour blood vessels and improve nanoparticle delivery. Nature Nanotechnology, 11(6), 533–538.* doi:10.1038/nnano.2015.342
6. White, S., Geubelle, P. Get ready for repair-and-go. Nature Nanotech **5,** 247–248 (2010). https://doi.org/10.1038/nnano.2010.66
7. Cingolani, R. The road ahead. Nature Nanotech **8,** 792–793 (2013). https://doi.org/10.1038/nnano.2013.238

8. Faria, M., Björnmalm, M., Thurecht, K.J. *et al.* Minimum information reporting in bio–nano experimental literature. *Nature Nanotech* **13,** 777–785 (2018). https://doi.org/10.1038/s41565-018-0246-4
9. Moscatelli, A. Nanoparticles go with the flow. Nature Nanotech (2013). https://doi.org/10.1038/nnano.2013.37
10. Toshiyuki Hayase, Numerical simulation of real-world flows, Fluid Dyn. Res. 47 (2015) 051201 (19pp), doi:10.1088/0169-5983/47/5/051201
11. Diez, F. J., Hernaiz, G., Miranda, J. J., & Sureda, M. (2013). *On the capabilities of nano electrokinetic thrusters for space propulsion. Acta Astronautica, 83, 97–107.* doi:10.1016/j.actaastro.2012.09.020
12. Borg, M. K., Lockerby, D. A., & Reese, J. M. (2015). *A hybrid molecular–continuum method for unsteady compressible multiscale flows. Journal of Fluid Mechanics, 768, 388–414.* doi:10.1017/jfm.2015.83
13. Wei Yu and Huaqing Xie, A Review on Nanofluids: Preparation, Stability Mechanisms, and Applications, Journal of Nanomaterials, Volume 2012, Article ID 435873, 17 pages doi:10.1155/2012/435873
14. Maxwell J C 1867 On the dynamical theory of gases Phil. Trans. R. Soc. 157 49 88
15. Abdelhamid Maali, Stéphane Colin, Bharat Bhushan. Slip length measurement of gas flow. Nanotechnology, Institute of Physics, 2016, 27 (37), pp.374004. 10.1088/0957-4484/27/37/374004, hal01392553
16. Majumder, M., Chopra, N., Andrews, R. & Hinds, B. J. Nanoscale hydrodynamics: enhanced flow in carbon nanotubes. Nature 438, 44 (2005).

17. Whitesides, G. M. (2006). *The origins and the future of microfluidics. Nature, 442(7101), 368–373.* doi:10.1038/nature05058
18. R. Qiao and N. R. Aluru, ``Charge inversion and flow reversal in a nanochannel electro-osmotic flow", *Physical Review Letters*, Vol. 92, No. 19, Art. No. 198301, 14 May 2004.
19. Cooper, S. M., Cruden, B. A., Meyyappan, M., Raju, R., & Roy, S. (2004). *Gas Transport Characteristics through a Carbon Nanotubue. Nano Letters, 4(2), 377–381.* doi:10.1021/nl0350682
20. Davarnejad, R., Barati, S. & Kooshki, M. CFD simulation of the effect of particle size on the nanofluids convective heat transfer in the developed region in a circular tube. SpringerPlus 2, 192 (2013). https://doi.org/10.1186/2193-1801-2-192
21. A.Kamyar, R.Saidur, M.Hasanuzzaman, Application of Computational Fluid Dynamics (CFD) for nanofluids, International Journal of Heat and Mass Transfer, Volume 55, Issues 15–16, July 2012, Pages 4104-4115, https://doi.org/10.1016/j.ijheatmasstransfer.2012.03.052
22. Liu, J., Cheng, S., Cao, N. *et al. Actinia*-like multifunctional nanocoagulant for single-step removal of water contaminants. *Nature Nanotech* **14,** 64–71 (2019). https://doi.org/10.1038/s41565-018-0307-8
23. Wei Yu and Huaqing Xie, A Review on Nanofluids: Preparation, Stability Mechanisms, and Applications, Journal of Nanomaterials, Volume 2012, Article ID 435873, 17 pages doi:10.1155/2012/435873
24. Frank J. Millero, Richard W. Curry, and Walter Drost-Hansen, Isothermal Compressibility of Water at Various Temperatures, Journal of Chemical and Engineering Data, Vol. 14, No. 4, October 1969, pp. 422-425, https://doi.org/10.1021/je60043a018

25. Rana A. Fine and Frank J. Millero, Compressibility of Water as a Function of Temperature and Pressure, AIP The Journal of Chemical Physics, 59(10):5529-5536, November 1973, DOI: 10.1063/1.1679903.

26. Brites, C., Xie, X., Debasu, M. *et al.* Instantaneous ballistic velocity of suspended Brownian nanocrystals measured by upconversion nanothermometry. *Nature Nanotech* **11,** 851–856 (2016). https://doi.org/10.1038/nnano.2016.111

27. Khan, N.S., Shah, Q., Bhaumik, A. et al. Entropy generation in bioconvection nanofluid flow between two stretchable rotating disks. Sci Rep **10,** 4448 (2020). https://doi.org/10.1038/s41598-020-61172-2

28. Tripathi, D., Bhushan, S., Bég, O.A. et al. Transient peristaltic diffusion of nanofluids: A model of micropumps in medical engineering. J Hydrodyn 30, 1001–1011 (2018). https://doi.org/10.1007/s42241-018-0140-4

29. HOYT, J. Laminar-turbulent transition in polymer solutions. *Nature* **270,** 508–509 (1977). https://doi.org/10.1038/270508a0

30. Novère, N. L. et al. Minimum information requested in the annotation of biochemical models (MIRIAM). Nat. Biotechnol. 23, 1509–1515 (2005).

31. J. Buongiorno, *Convective Transport in Nanofluids,* J. Heat Transfer. *Mar 2006, 128(3): 240-250 (11 pages) https://doi.org/10.1115/1.2150834*

32. Holland, D. M., Borg, M. K., Lockerby, D. A., & Reese, J. M. (2015). *Enhancing nano-scale computational fluid dynamics with molecular pre-simulations: Unsteady problems and design optimisation. Computers & Fluids, 115, 46–53.* doi:10.1016/j.compfluid.2015.03.023

33. Murray, C. D. The physiological principle of minimum work. I. The vascular system and the cost of blood volume. Proc. Natl Acad. Sci. USA 12, 207–214 (1926).

34. McCulloh, K. A., Sperry, J. S., & Adler, F. R. (2003). *Water transport in plants obeys Murray's law. Nature, 421(6926), 939–942.* doi:10.1038/nature01444

35. LaBarbera, M. Principles of design of fluid transport systems in zoology. Science 249, 992–999 (1990).

36. Singh, H., & Myong, R. S. (2018). *Critical Review of Fluid Flow Physics at Micro- to Nano-scale Porous Media Applications in the Energy Sector. Advances in Materials Science and Engineering, 2018, 1–31.* doi:10.1155/2018/9565240

37. Holland, D. M., Borg, M. K., Lockerby, D. A., & Reese, J. M. (2015). *Enhancing nano-scale computational fluid dynamics with molecular pre-simulations: Unsteady problems and design optimisation. Computers & Fluids, 115, 46–53.* doi:10.1016/j.compfluid.2015.03.023

38. Murray, C. D. The physiological principle of minimum work. I. The vascular system and the cost of blood volume. Proc. Natl Acad. Sci. USA 12, 207–214 (1926).

39. McCulloh, K. A., Sperry, J. S., & Adler, F. R. (2003). *Water transport in plants obeys Murray's law. Nature, 421(6926), 939–942.* doi:10.1038/nature01444

40. LaBarbera, M. Principles of design of fluid transport systems in zoology. Science 249, 992–999 (1990).

41. West, G. B., Brown, J. H. & Enquist, B. J. A general model for the structure and allometry of plant vascular systems. Nature 400, 664–667 (1999).

42. Tao, T. Searching for singularities in the Navier–Stokes equations. *Nat Rev Phys* 1, 418–419 (2019). https://doi.org/10.1038/s42254-019-0068-9

43. M. Moseler and U. Landman, Formation, stability, and breakup of nanojets, Science 289, 1165 (2000).
44. Chengxi Zhao, Duncan A. Lockerby, and James E. Sprittles, Dynamics of liquid nanothreads: Fluctuation-driven instability and rupture, Phys. Rev. Fluids 5, 044201 – Published 2 April 2020.
45. Wang, J & Joseph, D.D, "Boundary-layer analysis for effects of viscosity of the irrotational flow on the flow induced by a rapidly rotating cylinder in a uniform stream, J. Fluid Mech, Vol. 557, pp. 167–190, 2006, doi: 10.1017/s0022112006009670
46. Anderson, J. Jr., "Modern Compressible Flow, with Historical Perspective," Fourth Edition, McGraw-Hill Publishing Company, 2007
47. V R Sanal Kumar et al., Deflagration to Detonation Transition in Chemical Rockets with Sudden Expansion / Divergence Regions, AIAA Propulsion and Energy 2020 Forum, Innovative Propulsion Concepts, August 24-28, 2020, AIAA 2020-3520, https://doi.org/10.2514/6.2020-3520

Funding

This work was supported by SERB

Author Contributions

VRSK: conceptualization, analytical modeling, manuscript daft.

VS: Analytical modeling support and figures and tables preparation.

NC: Analytical modeling support and *in silico* verification

SARMR: Modeling support and table preparation

AS: Modeling support and *in silico* verification

RSB: Modeling support and *in vitro* verification

CO: *In vitro* verification and resources

PKR: Modeling support and intellectual input

SKC: Modeling support and intellectual input

Competing Interests: None

Authors have no competing interests as defined by your publications or other interests that might be perceived to influence the results and/or discussion reported in this paper.

Data and materials availability:

All data needed to evaluate the conclusions of the paper are available in the manuscript.

Disclosure Statement of Authors: Nothing to disclose

Declarations of interest: None

Disclosure Statement of Authors: Nothing to disclose

Table 1 Benchmark Data: Vigneshwaran's Table of Exact Solutions of Blockage Factor

Sl No.	Type of Gas	γ	Sanal Flow Choking Condition for *Diabatic Nano Flows*			LCDI *(CPR)*
			M_i	$\left(\frac{2\delta_x^*}{d_i}\right)$ 2D	$\left(\frac{2\delta_x^*}{d_i}\right)$ 3D	
1	Air	1.400	0.4374	0.3247	0.1782	1.8929
2	Argon	1.667	0.4236	0.3296	0.1812	2.0530
3	CO_2	1.289	0.4437	0.3224	0.1768	1.8257
4	Hydrogen	1.405	0.4372	0.3248	0.1783	1.8959
5	Methane	1.299	0.4431	0.3226	0.1770	1.8318
6	Neon	1.667	0.4236	0.3296	0.1812	2.0530
7	Octane	1.044	0.4587	0.3169	0.1735	1.6759

Table-II: Vigneshwaran's Table of Exact Solution

Air - $\gamma = 1.4$

Inlet Mach Number (M_i)	**Average Friction Coefficient ($\bar{f}$)**					
	$L^*/d_i = 27$	**$L^*/d_i = 28$**	**$L^*/d_i = 35$**	**$L^*/d_i = 85$**	**$L^*/d_i = 150$**	**$L^*/d_i = 300$**
0.02	16.467129	15.879017	12.703213	5.230735	2.964083	1.482042
0.04	4.077335	3.931716	3.145373	1.295154	0.733920	0.366960
0.06	1.787325	1.723492	1.378793	0.567738	0.321718	0.160859
0.08	0.988132	0.952841	0.762273	0.313877	0.177864	0.088932
0.1	0.619644	0.597514	0.478011	0.196828	0.111536	0.055768
0.12	0.420444	0.405428	0.324343	0.133553	0.075680	0.037840
0.14	0.301031	0.290280	0.232224	0.095621	0.054186	0.027093
0.16	0.224054	0.216052	0.172842	0.071170	0.040330	0.020165
0.18	0.171691	0.165559	0.132448	0.054537	0.030904	0.015452
0.2	0.134567	0.129761	0.103809	0.042745	0.024222	0.012111
0.22	0.107371	0.103536	0.082829	0.034106	0.019327	0.009663
0.24	0.086912	0.083808	0.067046	0.027607	0.015644	0.007822
0.26	0.071181	0.068639	0.054911	0.022610	0.012813	0.006406
0.28	0.058863	0.056761	0.045409	0.018698	0.010595	0.005298
0.3	0.049067	0.047315	0.037852	0.015586	0.008832	0.004416

Oxygen - $\gamma = 1.395$

Inlet Mach Number (M_i)	Average Friction Coefficient ($\bar{f}$)					
	$L^*/d_i = 27$	$L^*/d_i = 28$	$L^*/d_i = 35$	$L^*/d_i = 85$	$L^*/d_i = 150$	$L^*/d_i = 300$
0.02	16.526261	15.936037	12.748830	5.249518	2.974727	1.487363
0.04	4.092037	3.945893	3.156714	1.299823	0.736567	0.368283
0.06	1.793805	1.729740	1.383792	0.569797	0.322885	0.161442
0.08	0.991738	0.956318	0.765055	0.315023	0.178513	0.089256
0.10	0.621922	0.599711	0.479768	0.197552	0.111946	0.055973
0.12	0.422002	0.406931	0.325545	0.134048	0.075960	0.037980
0.14	0.302156	0.291364	0.233092	0.095979	0.054388	0.027194
0.16	0.224899	0.216867	0.173493	0.071438	0.040482	0.020241
0.18	0.172345	0.166190	0.132952	0.054745	0.031022	0.015511
0.20	0.135084	0.130260	0.104208	0.042909	0.024315	0.012158
0.22	0.107787	0.103938	0.083150	0.034238	0.019402	0.009701
0.24	0.087252	0.084136	0.067309	0.027715	0.015705	0.007853
0.26	0.071463	0.068911	0.055129	0.022700	0.012863	0.006432
0.28	0.059099	0.056988	0.045590	0.018772	0.010638	0.005319
0.30	0.049265	0.047506	0.038005	0.015649	0.008868	0.004434

Carbon Dioxide – $\gamma = 1.289$

Inlet Mach Number (M_i)	Average Friction Coefficient ($\bar{f}$)					
	$L^*/d_i = 27$	$L^*/d_i = 28$	$L^*/d_i = 35$	$L^*/d_i = 85$	$L^*/d_i = 150$	$L^*/d_i = 300$
0.02	17.887824	17.248973	13.799179	5.682015	3.219808	1.609904
0.04	4.430553	4.272319	3.417855	1.407352	0.797500	0.398750
0.06	1.943020	1.873627	1.498901	0.617195	0.349744	0.174872
0.08	1.074778	1.036393	0.829115	0.341400	0.193460	0.096730
0.10	0.674383	0.650298	0.520238	0.214216	0.121389	0.060694
0.12	0.457886	0.441533	0.353226	0.145446	0.082420	0.041210
0.14	0.328069	0.316353	0.253082	0.104210	0.059053	0.029526
0.16	0.244361	0.235634	0.188507	0.077621	0.043985	0.021992
0.18	0.187399	0.180706	0.144565	0.059527	0.033732	0.016866
0.20	0.146998	0.141748	0.113398	0.046693	0.026460	0.013230
0.22	0.117388	0.113196	0.090556	0.037288	0.021130	0.010565
0.24	0.095103	0.091706	0.073365	0.030209	0.017118	0.008559
0.26	0.077959	0.075175	0.060140	0.024763	0.014033	0.007016
0.28	0.064526	0.062222	0.049778	0.020497	0.011615	0.005807
0.30	0.053838	0.051915	0.041532	0.017101	0.009691	0.004845

Nitrogen - $\gamma = 1.4$

Inlet Mach Number (M_i)	Average Friction Coefficient ($\bar{f}$)					
	$L^*/d_i = 27$	$L^*/d_i = 28$	$L^*/d_i = 35$	$L^*/d_i = 85$	$L^*/d_i = 150$	$L^*/d_i = 300$
0.02	16.467129	15.879017	12.703213	5.230735	2.964083	1.482042
0.04	4.077335	3.931716	3.145373	1.295154	0.733920	0.366960
0.06	1.787325	1.723492	1.378793	0.567738	0.321718	0.160859
0.08	0.988132	0.952841	0.762273	0.313877	0.177864	0.088932
0.1	0.619644	0.597514	0.478011	0.196828	0.111536	0.055768
0.12	0.420444	0.405428	0.324343	0.133553	0.075680	0.037840
0.14	0.301031	0.290280	0.232224	0.095621	0.054186	0.027093
0.16	0.224054	0.216052	0.172842	0.071170	0.040330	0.020165
0.18	0.171691	0.165559	0.132448	0.054537	0.030904	0.015452
0.2	0.134567	0.129761	0.103809	0.042745	0.024222	0.012111
0.22	0.107371	0.103536	0.082829	0.034106	0.019327	0.009663
0.24	0.086912	0.083808	0.067046	0.027607	0.015644	0.007822
0.26	0.071181	0.068639	0.054911	0.022610	0.012813	0.006406
0.28	0.058863	0.056761	0.045409	0.018698	0.010595	0.005298
0.3	0.049067	0.047315	0.037852	0.015586	0.008832	0.004416

Helium – $\gamma = 1.667$

Inlet Mach Number (M_i)	Average Friction Coefficient ($\bar{f}$)					
	$L^*/d_i = 27$	$L^*/d_i = 28$	$L^*/d_i = 35$	$L^*/d_i = 85$	$L^*/d_i = 150$	$L^*/d_i = 300$
0.02	13.824736	13.330996	10.664797	4.391387	2.488453	1.244226
0.04	3.420418	3.298260	2.638608	1.086486	0.615675	0.307838
0.06	1.497793	1.444300	1.155440	0.475769	0.269603	0.134801
0.08	0.827028	0.797491	0.637993	0.262703	0.148865	0.074433
0.10	0.517887	0.499391	0.399513	0.164505	0.093220	0.046610
0.12	0.350858	0.338328	0.270662	0.111449	0.063154	0.031577
0.14	0.250794	0.241837	0.193469	0.079664	0.045143	0.022571
0.16	0.186338	0.179683	0.143746	0.059190	0.033541	0.016770
0.18	0.142529	0.137438	0.109951	0.045274	0.025655	0.012828
0.20	0.111499	0.107516	0.086013	0.035417	0.020070	0.010035
0.22	0.088790	0.085619	0.068495	0.028204	0.015982	0.007991
0.24	0.071727	0.069165	0.055332	0.022784	0.012911	0.006455
0.26	0.058623	0.056530	0.045224	0.018622	0.010552	0.005276
0.28	0.048376	0.046649	0.037319	0.015367	0.008708	0.004354
0.30	0.040239	0.038802	0.031042	0.012782	0.007243	0.003622

Figures

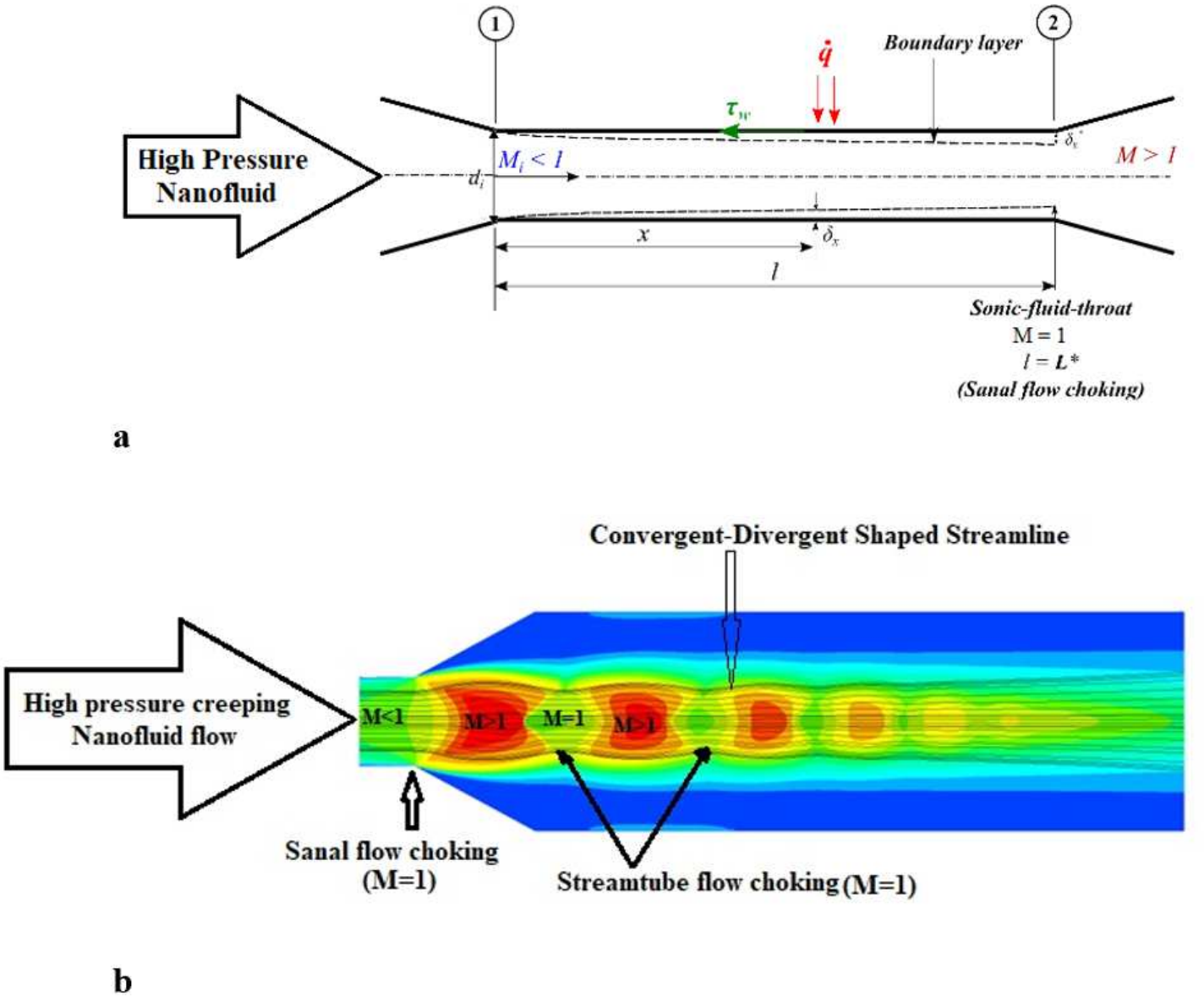

Figure 1

(a) Demonstrating the Sanal flow choking condition in an idealized physical model of an internal nanoscale fluid flow system. (b) Demonstrating the Sanal flow choking and streamtube flow choking condition in an idealized physical model of an internal nanoscale fluid flow system.

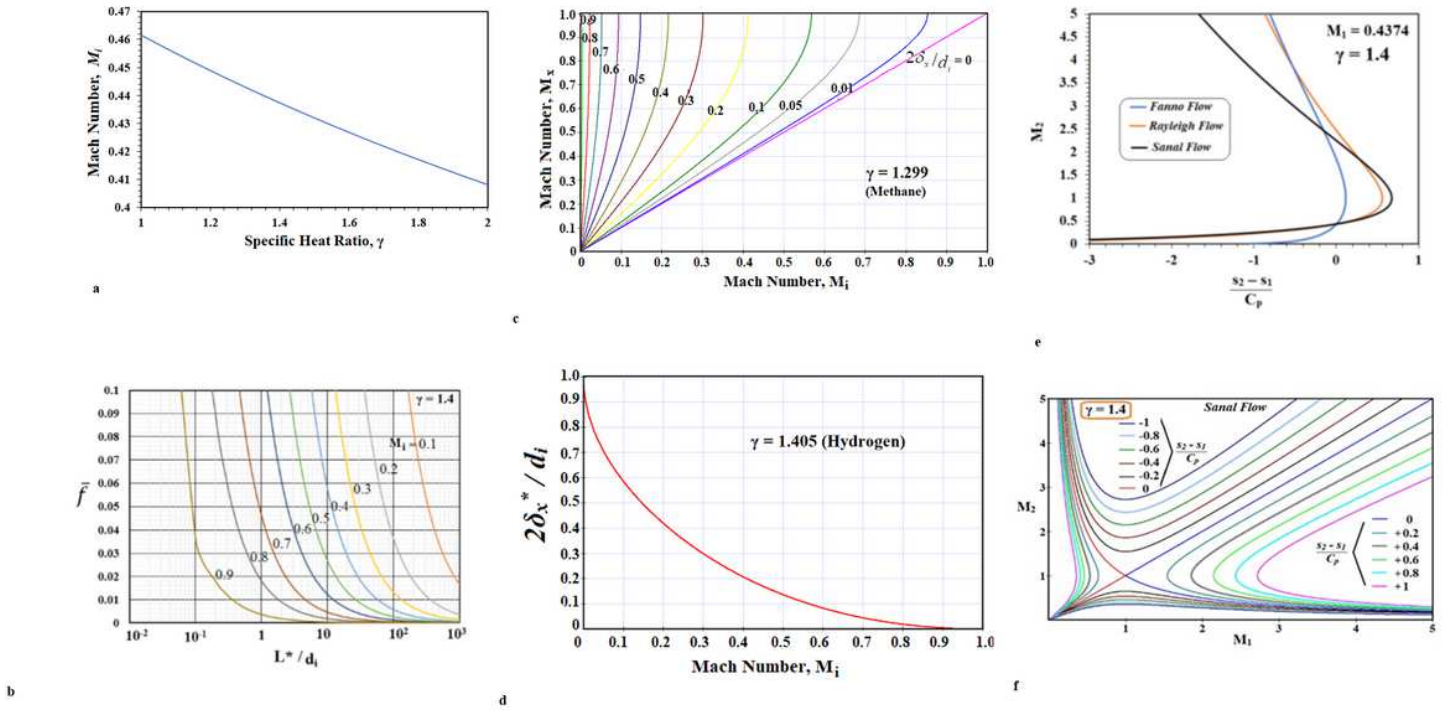

Figure 2

(a) Inlet Mach number prediction of different gases with different HCR (γ) for achieving Sanal flow choking condition for diabatic nanoflows. (b) Analytical prediction of the average friction coefficient at the Sanal flow choking condition of different nanotubes at different inlet conditions. (c) The solution curve of Eq.2(a) showing the 3D blockage factor with Methane as the working fluid. (d) The solution curve of Eq.2(b) showing the 3D blockage factor at the sonic-fluid-throat of a nanofluid flow system with hydrogen as the working fluid. (e) Mach Number-Entropy chart of Fanno, Rayleigh and Sanal flow models at the choked flow condition. (f). The demonstration of the Sanal flow choking in diabatic nanofluid flows. (Solution curves of Eq. 6).